Phase Noise in Externally Injection-Locked Oscillator Arrays

Heng-Chia Chang, Xudong Cao, Mark J. Vaughan, *Member, IEEE*,
Umesh K. Mishra, and Robert A. York, *Member, IEEE*

***Abstract*— Previous investigations of noise in mutually synchronized coupled-oscillator systems are extended to include the effects of phase noise introduced by externally injected signals. The analysis is developed for arbitrarily coupled arrays and an arbitrary collection of coherent injected signals, and is illustrated with the specific case of linear chains of nearest neighbor coupled oscillators either globally locked (locking signal applied to each array element) or with the locking signal applied to a single-array element. It is shown that the general behavior is qualitatively similar to a single injection-locked oscillator, with the output noise tracking the injected noise near the carrier, and returning to the free-running array noise far from the carrier, with intermediate behavior significantly influenced by the number of array elements and injection strength. The theory is validated using a five-element GaAs MESFET oscillator array operating at X-band.**

***Index Terms*— Array noise, globally locked, injection locked, injection strength, noise admittance, noise offset frequency, phase noise, power spectral density, single element locked, synchronization.**

I. Introduction

COUPLED oscillator systems possess synchronization properties that may be suitable for certain millimeter-wave power-combining and beam-scanning applications [1]. In previous analytical and experimental work it has been shown that robust locking favors a low-Q oscillator design, which implies a large locking range. Unfortunately, low-Q factors also imply larger phase noise. In [2], the authors showed that the phase noise in a mutually synchronized oscillator array is reduced in comparison to a single-array element by a factor of N, where N is the number of array elements. For many applications and reasonable array sizes, this reduction is still insufficient to meet system requirements. External locking to a low-noise source is a possible solution. This paper extends our previous work to include the effects of noise introduced by an external locking signal, and explores the spectral characteristics of the noise and the dependence on array size and external locking configuration for a practical nearest neighbor coupled-oscillator system. Only phase noise is considered; amplitude noise and A.M.-to-P.M. noise conversion are assumed negligibly small in comparison to the P.M. noise [3] in this paper.

Manuscript received March 19, 1997; revised July 18, 1997. This work was supported by Hughes Research Laboratories, Malibu, CA, under a California MICRO Grant.

H.-C. Chang, X. Cao, U. K. Mishra, and R. A. York are with the Department of Electrical and Computer Engineering, University of California at Santa Barbara (UCSB), CA, 93106 USA.

M. J. Vaughan is with the Endgate Corporation, Sunnyvale, CA 94086 USA.

Publisher Item Identifier S 0018-9480(97)08017-4.

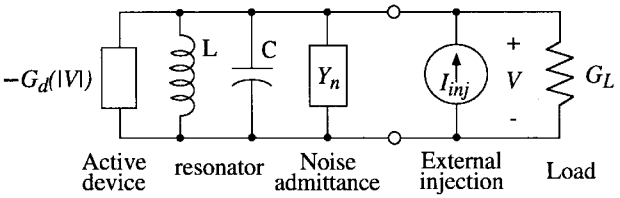

Fig. 1. Single-resonant negative-conductance oscillator model used in this paper. Phase noise is modeled by a fluctuating susceptance, as in [4].

II. A Single Noisy Oscillator with a Noisy Injected Signal

It will prove convenient to first review the noise properties of a single injection-locked oscillator. This will provide an example of the method of attack, and the results will be used as a baseline for comparison with more complicated array noise results.

The oscillator model used in this paper is shown in Fig. 1. Each oscillator has a negative conductance device, a resonator, and a complex noise admittance [4]. If the oscillator is under-injection locked to the external source, the phase relationship between the oscillator and the injection source can be described as [1], [2], [5], [6]:

$$\frac{d\theta}{dt} = \omega_0 - \frac{\omega_o \rho}{2Q}\sin(\theta - \psi_{\text{inj}}) - \frac{\omega_0}{2Q}B_n(t) \tag{1}$$

where $\theta, \psi_{\text{inj}}$ are the instantaneous phases of the oscillator and injection signals, respectively, and ω_0 and Q are the free-running frequency and Q factor of the oscillators, respectively. $\rho = A_{\text{inj}}/A$ is the injection strength (i.e., the injection signal A_{inj} is normalized to the oscillator's free-running amplitude A). $B_n(t)$ is a time-varying noise susceptance (or the quadrature-phase component of the noise admittance), assumed to be an ergodic process [4]. A steady-state noise-free synchronized state satisfies

$$\sin(\hat{\theta} - \hat{\psi}_{\text{inj}}) = \frac{\omega_0 - \omega_{\text{inj}}}{\rho\omega_{3\,\text{dB}}} = \frac{\omega_0 - \omega_{\text{inj}}}{\Delta\omega_{\text{lock}}} \tag{2}$$

where $\omega_{\text{inj}} = d\theta/dt$ is the injection frequency, $\omega_{3\,\text{dB}} \equiv \omega_0/2Q$ is half the 3-dB bandwidth of the oscillator tank circuits, $\Delta\omega_{\text{lock}} = \rho\omega_{3\,\text{dB}}$ is half the entire locking range, and the circumflex ($\hat{}$) denotes a steady-state quantity. Assuming the noise is a small perturbation to the noise-free solution, we

write $\theta \rightarrow \hat{\theta} + \delta\theta$ and $\psi_{\rm inj} \rightarrow \hat{\psi}_{\rm inj} + \delta\psi_{\rm inj}$, where $\delta\theta$ and $\delta\psi_{\rm inj}$ describe the small phase fluctuations of the oscillator and injected signal, and (1) becomes

$$\frac{1}{\omega_{3\,\rm dB}}\frac{d\delta\theta}{dt} = -\rho\cos(\hat{\theta} - \hat{\psi}_{\rm inj})(\delta\theta - \delta\psi_{\rm inj}) - B_n(t). \quad (3)$$

Fourier transforming (3) and rearranging terms gives

$$\tilde{\delta\theta} = \frac{\rho\cos(\hat{\theta} - \hat{\psi}_{\rm inj})}{\jmath(\omega/\omega_{3\,\rm dB}) + \rho\cos(\hat{\theta} - \hat{\psi}_{\rm inj})}\tilde{\delta\psi} - \frac{1}{\jmath(\omega/\omega_{3\,\rm dB}) + \rho\cos(\hat{\theta} - \hat{\psi}_{\rm inj})}\tilde{B}_n. \quad (4)$$

The tilde ($\tilde{}$) denotes a transformed or spectral variable, and ω is the noise frequency measured relative to the carrier. The power spectrum of the oscillator phase fluctuation is then computed from $\langle\tilde{\delta\theta}\cdot\tilde{\delta\theta}^*\rangle$, where the notation $\langle\ \rangle$ represents an ensemble average. Evaluating this power spectra using (4) leads to cross-power spectral densities of the form $\langle\tilde{B}_n\tilde{\delta\psi}^*_{\rm inj}\rangle$, which vanish, assuming $B_n(t)$ and $\delta\psi_{\rm inj}(t)$ are uncorrelated random processes with zero time average. In the absence of an injected signal, the power spectral density of the oscillator phase fluctuations (the phase noise) reduces to the familiar [2]

$$|\tilde{\delta\theta}|^2 \Rightarrow |\tilde{\delta\theta}_0|^2 \equiv |\tilde{\delta\theta}_i|^2_{\rm uncoupled} = \frac{|\tilde{B}_n|^2}{(\omega/\omega_{3\,\rm dB})^2}. \quad (5)$$

We then find

$$|\tilde{\delta\theta}|^2 = \frac{(\omega/\omega_{3\,\rm dB})^2|\tilde{\delta\theta}_0|^2}{(\omega/\omega_{3\,\rm dB})^2 + \rho^2\cos^2(\hat{\theta} - \hat{\psi}_{\rm inj})} + \frac{\rho^2\cos^2(\hat{\theta} - \hat{\psi}_{\rm inj})|\tilde{\delta\psi}_{\rm inj}|^2}{(\omega/\omega_{3\,\rm dB})^2 + \rho^2\cos^2(\hat{\theta} - \hat{\psi}_{\rm inj})} \quad (6)$$

where we have dropped the $\langle\ \rangle$ notation, an ensemble or time average being implicitly understood. The result (6) is essentially the same as that derived by Kurokawa [7], and has been discussed extensively by Day *et al.* [8]. The essential features are: 1) the near-carrier noise is approximately that of the injected signal over most of the locking range, but approaches that of the free-running oscillator at the band edges ($\hat{\theta} - \hat{\psi}_{\rm inj} \approx \pi/2$) and 2) the noise far from the carrier is that of the free-running oscillator.

III. Coupled Oscillators with External Locking Sources

We now consider arrays of oscillators of the general form shown in Fig. 2, where each oscillator is again assumed to be modeled as in Fig. 1. The oscillators are coupled in parallel using a coupling network described by Y-parameters (see [9] for a discussion of the influence of the oscillator equivalent circuit). This model is similar to that used in previous work with the exception of the addition of independent sources at each port to account for externally injected signals from a locking source. These sources are assumed to be mutually coherent at a frequency $\omega_{\rm inj}$, but can have arbitrary amplitude and phase. Using methods from earlier work [1], we find that

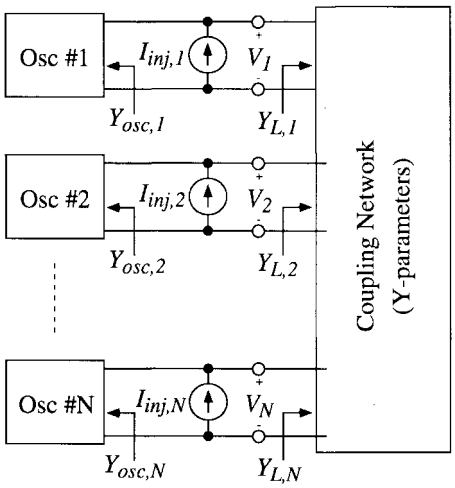

Fig. 2. Oscillators coupled in parallel through an arbitrary network described by Y-parameters. A set of mutually coherent sources apply injected signals at each port.

the phase dynamics of an N-element array are predominantly governed by

$$\frac{d\theta_i}{dt} = \omega_i - \frac{\omega_i}{2Q}\left[\sum_{j=1}^{N}\mathrm{Im}\{\kappa_{ij}e^{\jmath(\theta_j-\theta_i)}\} + \rho_i\sin(\theta_i - \psi_i) + B_{ni}(t)\right] \quad (7)$$

for $i = 1, 2, \cdots, N$, where the following parameters have been used to describe the ith oscillator:

- ω_i free-running frequency;
- θ_i instantaneous phase;
- ρ_i normalized injected signal amplitude;
- ψ_i instantaneous phase of injected signal;
- B_{ni} noise susceptance;
- Q Q factor.

We have also assumed the oscillator amplitudes are approximately the same in (7). The coupling parameters κ_{ij} are defined by

$$\kappa_{ij} = \frac{Y_{ij}}{G_L} = \epsilon_{ij}e^{\jmath(\pi - \Phi_{ij})} \quad (8)$$

where Y_{ij} describe the admittance or Y-parameters of the coupling network, and G_L is the load conductance required for the free-running oscillator to achieve the desired oscillation amplitude. The coupling strength and coupling delay between oscillators are given by ϵ_{ij} and Φ_{ij}, respectively. Our approach to noise analysis involves examining the perturbations in the phases brought about by the independent noise sources in each oscillator, modeled by the ergodic processes $B_{ni}(t)$. These phase fluctuations are assumed to be small, which enables us to linearize the nonlinear equations around a steady-state *noiseless* solution. Therefore, it is necessary to first quantify the steady-state noiseless solutions in the presence of external locking signals.

For simplicity, we will restrict attention to systems with reciprocal nearest neighbor coupling. This is an important

class of oscillator arrays from both a practical and analytical standpoint, and based on previous work [2], we expect the results to be representative of most reciprocally coupled arrays. The coupling parameters in this case are

$$\kappa_{ij} = \begin{cases} 1, & i = j \\ \epsilon e^{j(\pi - \Phi)}, & |i-j| = 1 \\ 0, & \text{otherwise} \end{cases} \tag{9}$$

where ϵ defines the strength of the coupling, and Φ describes the inter-oscillator coupling phase delay. We have also previously argued [9] for the design of coupling networks so that $\Phi \approx n\pi$, where n is an integer. Assuming this to be the case, and noting that $\Phi = 2n\pi$ is appropriate for the formulation (7), the noiseless steady-state phases $\hat{\theta}_i$ must satisfy

$$\omega_{\text{inj}} = \omega_i - \omega_{3\,\text{dB}}[\epsilon \sin(\hat{\theta}_{i-1} - \hat{\theta}_i) + \epsilon \sin(\hat{\theta}_{i+1} - \hat{\theta}_i) + \rho_i \sin(\hat{\theta}_i - \psi_i)], \qquad i = 1, 2, \cdots, N \tag{10}$$

where $\omega_{3\,\text{dB}} \equiv \omega_i/2Q$ is half the 3-dB bandwidth of the oscillator resonant circuits, and the terms involving θ_0 or θ_{N+1} (encountered for the end elements in the array, $i = 1$ or N) are to be ignored.

We have previously studied this equation extensively for the case when there are no externally injected signals ($\rho_i = 0$). Generally, a desired phase distribution can be assumed and substituted into (10) to find the conditions for maintaining this phase (the distribution must also be checked for stability). We have found that a constant phase progression can be established along the array so that $\hat{\theta}_i - \hat{\theta}_{i-1} = \Delta\theta$, by properly selecting the free-running frequencies ω_i, which are typically controlled by a dc voltage across a varactor embedded in the oscillator circuits. This phase progression is a stable solution provided that

$$-90^\circ < \Delta\theta < 90^\circ. \tag{11}$$

This solution is established by setting all of the free-running frequencies of the central-array elements to a common center frequency, and slightly detuning the peripheral elements in proportion to the amount of desired inter-element phase shift. The uniform phase distribution is a common design objective, and potentially useful for beam scanning or power combining.

Examining (10) when $\rho_i \neq 0$, we find that the competing effects of injection locking and mutual coupling tend to preclude uniform phase progressions unless: 1) the phasing of the injected signals is identical with that arising from mutual coupling, and so tends to reinforce the solution described above or 2) only a single-array element is injection locked. These are very general observations; there may be special circumstances where careful adjustment of all the free-running frequencies and phasing of the injected signals may lead to desirable phase distributions, but these solutions are difficult to analytically quantify due to the nonlinear nature of the equations. Therefore, in our treatment of noise, we will apply the results to the following two cases which appear to have practical merit. We assume each oscillator feeds an antenna, so that injected signals can be applied quasi-optically or via local circuits as follows.

- *Case 1:* Global illumination of the array with $\rho_i = \rho$ and $\psi_i - \psi_{i-1} = \Delta\psi$, as shown in Fig. 3(a), with the free-running frequencies adjusted so that $\Delta\theta = \Delta\psi$. In this case, the incident locking beam and the mutual coupling act in concert to produce an output beam emerging as if specularly reflected. The system thus resembles a quasi-optical injection-locked amplifier. The injected signal establishes a common phase reference, which we define as $\psi_1 = 0$. If the central array elements are adjusted so that $\omega_i = \omega_{\text{inj}}$, then the above assumptions are satisfied by

$$\omega_i = \begin{cases} \omega_{\text{inj}} + \Delta\omega_{\text{lock}} \sin\Delta\psi, & i = 1 \\ \omega_{\text{inj}}, & 1 < i < N \\ \omega_{\text{inj}} - \Delta\omega_{\text{lock}} \sin\Delta\psi, & i = N \end{cases} \tag{12}$$

  which is independent of the locking signal strength, and is the same condition required to establish a uniform phase progression in a mutually synchronized array with no locking [1]. We have also defined $\Delta\omega_{\text{lock}} \equiv \epsilon\omega_{3\,\text{dB}}$ in (12). Using methods described in [1], it can be shown that this mode is stable as long as (11) holds.
- *Case 2:* A single element of the array locked to an external source, as shown in Fig. 3(b), with the free running frequencies adjusted to produce a uniform phase progression $\Delta\theta$. If the ℓth element is externally locked, we write $\rho_i = \rho\delta_{\ell i}$, where δ_{ij} is the Kronecker delta, and $\psi_\ell = 0$ is the phase reference for the system. Here

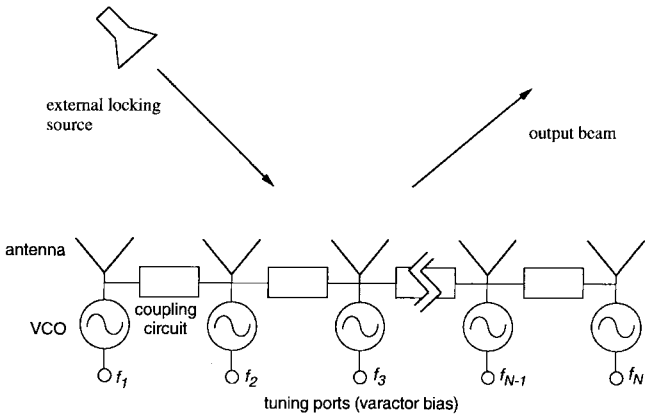

(a)

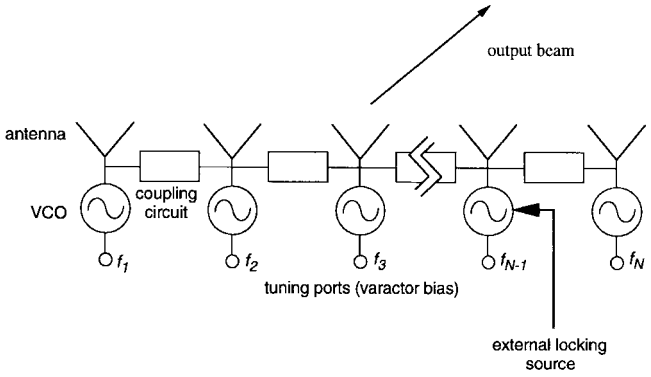

(b)

Fig. 3. Two specific cases considered in this paper to illustrate the general theory. (a) Globally injection-locked array (Case 1), with the locking signal applied quasi-optically and (b) array with single element locked to an external source (Case 2).

we can distinguish between external locking of a central-array element and an end element ($i = 1$ or $i = N$) of the array. In the former case, we find that a valid free-running frequency distribution is given by (12) with $\Delta\psi = \Delta\theta$. When an end-element is locked, we find (for $\ell = 1$)

$$\omega_i = \begin{cases} \omega_{\rm inj} + \omega_{3\,\rm dB}[\epsilon \sin\Delta\theta - \rho \sin\hat{\theta}_1], & i = 1 \\ \omega_{\rm inj}, & 1 < i < N \\ \omega_{\rm inj} - \Delta\omega_{\rm lock} \sin\Delta\theta, & i = N. \end{cases} \tag{13}$$

If we choose $\rho = \epsilon$ and $\hat{\theta}_1 = \Delta\theta$, then the output beam is controlled only by a single frequency variable, or equivalently, a single dc voltage.

IV. Array Noise Analysis

Once a steady-state solution for the phase distribution has been computed, the dynamic equation (7) is used to investigate the behavior of small fluctuations around the steady-state solution. Making the substitutions $\theta_i \to \hat{\theta}_i + \delta\theta_i$ and $\psi_i \to \hat{\psi}_i + \delta\psi_{\rm inj}$, and assuming $\delta\theta_i$ and $\delta\psi_{\rm inj}$ are small, gives

$$-\frac{1}{\omega_{3\,\rm dB}}\frac{d\delta\theta_i}{dt} = \sum_{j=1}^{N} \epsilon_{ij}(\delta\theta_i - \delta\theta_j)\cos(\hat{\theta}_i - \hat{\theta}_j + \Phi_{ij}) + \rho_i(\delta\theta_i - \delta\psi_{\rm inj})\cos(\hat{\theta}_i - \hat{\psi}_i) + B_{ni}(t). \tag{14}$$

Note that all of the injected signals are assumed to be derived from the same source, and, therefore, all share a common time-dependent fluctuation $\psi_{\rm inj}$ (we assume that any relative delays in the paths of the injected signals are short compared with the coherence length of the injection source). Taking the Fourier transform and rearranging some terms gives

$$\sum_{j=1}^{N} \epsilon_{ij}(\widetilde{\delta\theta}_j - \widetilde{\delta\theta}_i)\cos(\hat{\theta}_i - \hat{\theta}_j + \Phi_{ij}) - \jmath\frac{\omega}{\omega_{3\,\rm dB}}\widetilde{\delta\theta}_i - \rho_i\widetilde{\delta\theta}_i\cos(\hat{\theta}_i - \hat{\psi}_i) = \tilde{B}_{ni} - \rho_i\widetilde{\delta\psi}_{\rm inj}\cos(\hat{\theta}_i - \hat{\psi}_i) \tag{15}$$

where the tilde ($\tilde{}$) denotes a transformed or spectral variable, and ω is the noise frequency measured relative to the carrier. This equation can be written in matrix form. Using a similar notation as in [2]:

$$\overline{\overline{N}} \cdot \overline{\widetilde{\delta\theta}} = \overline{\tilde{B}_n} - \widetilde{\delta\psi}_{\rm inj}\overline{\rho'} \tag{16}$$

where

$$\overline{\widetilde{\delta\theta}} = \begin{pmatrix} \widetilde{\delta\theta}_1 \\ \widetilde{\delta\theta}_2 \\ \vdots \\ \widetilde{\delta\theta}_N \end{pmatrix} \quad \overline{\tilde{B}_n} = \begin{pmatrix} \tilde{B}_{n1} \\ \tilde{B}_{n2} \\ \vdots \\ \tilde{B}_{nN} \end{pmatrix}$$

$$\overline{\rho'} = \begin{pmatrix} \rho_1\cos(\hat{\theta}_1 - \hat{\psi}_1) \\ \rho_2\cos(\hat{\theta}_2 - \hat{\psi}_2) \\ \vdots \\ \rho_N\cos(\hat{\theta}_N - \hat{\psi}_N) \end{pmatrix}.$$

The phase fluctuations of the individual oscillator are then determined by inverting (16):

$$\overline{\widetilde{\delta\theta}} = \overline{\overline{P}} \cdot \overline{\tilde{B}_n} - \widetilde{\delta\psi}_{\rm inj}\overline{\overline{P}} \cdot \overline{\rho'} \tag{17}$$

where $\overline{\overline{P}} = \overline{\overline{N}}^{-1}$, so that

$$\widetilde{\delta\theta}_i = \sum_{j=1}^{N} p_{ij}\tilde{B}_{nj} - \widetilde{\delta\psi}_{\rm inj}\sum_{j=1}^{N} p_{ij}\rho'_j \tag{18}$$

where p_{ij} is an element of the matrix $\overline{\overline{P}}$.

The combined output of all the array elements is the most important quantity of interest in coupled-oscillator array applications. In previous work [2], we showed that the total phase fluctuation of the combined output signal

$$\widetilde{\delta\theta}_{\rm total} = \frac{1}{N}\sum_{j=1}^{N}\widetilde{\delta\theta}_j. \tag{19}$$

Using (18), we can write (19) as

$$\widetilde{\delta\theta}_{\rm total} = \frac{1}{N}\sum_{j=1}^{N}\sum_{i=1}^{N} p_{ij}\tilde{B}_{nj} - \frac{\widetilde{\delta\psi}_{\rm inj}}{N}\sum_{j=1}^{N}\sum_{i=1}^{N} p_{ij}\rho'_j. \tag{20}$$

The power spectral density of the total phase fluctuation (i.e., the phase noise) is computed as described in [2], assuming the internal noise sources of the oscillators have the same power spectral density, but mutually uncorrelated, and are also uncorrelated with the injected signal noise, which leads to a total phase noise described by

$$|\widetilde{\delta\theta}_{\rm total}|^2 = \frac{|\tilde{B}_n|^2}{N^2}\sum_{j=1}^{N}\left|\sum_{i=1}^{N} p_{ij}\right|^2 + \frac{|\widetilde{\delta\psi}_{\rm inj}|^2}{N^2}\left|\sum_{j=1}^{N}\sum_{i=1}^{N} p_{ij}\rho'_j\right|^2. \tag{21}$$

The first term is the contribution from all the internal noise sources, including the effects of the mutual coupling. The second term is the contribution from the noise of the external injection source. For a given coupling network and injection-locking configuration, the task of noise analysis is reduced to that of computing the matrix elements p_{ij}. As discussed in [2], in some cases, these sums can be analytically resolved.

A. Globally Injected Array

The inverse of $\overline{\overline{N}}$ is not easily expressed for the general case, even for relatively simple coupling topologies. However, note that from the relation $\overline{\overline{P}} \cdot \overline{\overline{N}} = \overline{\overline{N}} \cdot \overline{\overline{P}} = \overline{\overline{I}}$ we can write

$$\sum_{j=1}^{N} n_{ij}p_{jk} = \delta_{ik}$$

$$\sum_{i=1}^{N}\sum_{j=1}^{N} n_{ij}p_{jk} = \sum_{j=1}^{N} p_{jk}\left(\sum_{i=1}^{N} n_{ij}\right) = 1. \tag{22}$$

For the general case, the matrix elements n_{ij} are known in closed form, and it can be shown that

$$\sum_{i=1}^{N} n_{ij} = \sum_{k=1}^{N} \epsilon_{jk}\sin(\Phi_{jk})\sin(\hat{\theta}_j - \hat{\theta}_k) - \frac{\jmath\omega}{\omega_{3\rm dB}} - \rho_j\cos(\hat{\theta}_j - \hat{\psi}_j). \tag{23}$$

Substituting the conditions for a globally illuminated array as described earlier (Case 1, i.e., $\rho_j = \rho, \widehat{\theta}_j - \widehat{\psi}_j = 2n\pi$, and $\Phi = 2n\pi$, where n is an integer), we find

$$\sum_{i=1}^{N} n_{ij} = -\frac{\jmath\omega}{\omega_{3\text{dB}}} - \rho \tag{24}$$

and so, from (22)

$$\sum_{j=1}^{N} p_{jk} = \frac{-1}{\rho + \jmath\omega/\omega_{3\text{dB}}}. \tag{25}$$

The total output noise from (21) is then

$$|\widetilde{\delta\theta}_{\text{total}}|^2 = \frac{1}{N}|\widetilde{\delta\theta}_0|^2 \frac{(\omega/\omega_{3\text{dB}})^2}{\rho^2 + (\omega/\omega_{3\text{dB}})^2} + |\widetilde{\delta\psi}_{\text{inj}}|^2 \frac{\rho^2}{\rho^2 + (\omega/\omega_{3\text{dB}})^2} \tag{26}$$

where the term $|\widetilde{\delta\theta}_0|^2$ is the noise of a single free-running oscillator from (5). The total noise has exactly the same form as the result obtained for a single injection-locked oscillator (6), except that the contribution from internal noise sources in the array is reduced by $1/N$, which is the same result as found in [2], in the absence of injected signals. Near the carrier, the output noise is that of the injected signal

$$\lim_{\omega\to 0} |\widetilde{\delta\theta}_{\text{total}}|^2 = |\widetilde{\delta\psi}_{\text{inj}}|^2 \tag{27}$$

and far from the carrier the noise reduces to that of a free-running synchronized array as follows:

$$\lim_{\omega\to\infty} |\widetilde{\delta\theta}_{\text{total}}|^2 = \frac{1}{N}|\widetilde{\delta\theta}_0|^2. \tag{28}$$

The spectral characteristics of the total noise in (26) for intermediate frequencies are shown in Fig. 4 for several array sizes, assuming $\epsilon = 0.1, \rho = 0.02$, and both the internal and injected noise characteristics follow the ideal $1/f^2$ dependence. The individual array elements were taken to have a single sideband noise of -60 dBc/Hz @100-kHz offset, typical of a low-Q microstrip MESFET oscillator, and the injection source was modeled by a similar noise source with -130 dBc/Hz @100-kHz offset. Note that the noise characteristics improve slightly with increasing array size, which is due to the $1/N$ reduction of the contribution from the internal noise sources, arising from mutual coupling in the array. The dependence on the injected signal strength for the same parameters described above is also shown in Fig. 5.

B. Array with One Element Externally Locked

Following a similar analysis for the case of a single-array element coupled to an external locking source (Case 2, i.e., $\rho_j = \rho\delta_{\ell j}, \widehat{\theta}_j - \widehat{\psi}_j = 2n\pi$, and $\Phi = 2n\pi$, where n is an integer), we find, for a signal applied to the ℓth element

$$\sum_{i=1}^{N} n_{ij} = -\frac{\jmath\omega}{\omega_{3\text{dB}}} - \rho\delta_{\ell j} \tag{29}$$

which gives, from (22)

$$-\frac{\jmath\omega}{\omega_{3\text{dB}}} \sum_{j=1}^{N} p_{jk} - \rho p_{\ell k} = 1, \qquad k = 1, 2, \cdots, N. \tag{30}$$

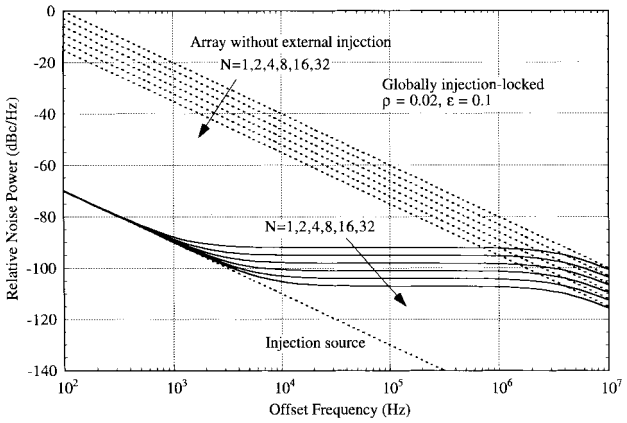

Fig. 4. Spectral characteristics of the phase noise in a globally illuminated array [Fig. 3(a)] for several array sizes, both with (solid line) and without (dotted line) the injected signal. The noise characteristics slightly improve with increasing array size due to the mutual coupling.

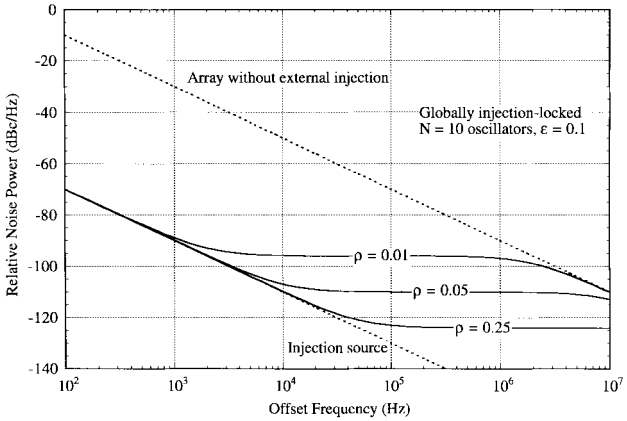

Fig. 5. Spectral characteristics of the phase noise in a globally illuminated array [Fig. 3(a)] versus normalized injection strength for the specific case of $N = 10$.

The total noise is then given by

$$|\widetilde{\delta\theta}_{\text{total}}|^2 = \frac{|\widetilde{\delta\theta}_0|^2}{N^2} \sum_{j=1}^{N} |1 + \rho p_{\ell j}|^2 + \rho^2 \frac{|\widetilde{\delta\psi}_{\text{inj}}|^2}{N^2} \left| \sum_{i=1}^{N} p_{\ell j} \right|^2 \tag{31}$$

where the property $p_{ij} = p_{ji}$ was used. We cannot evaluate this expression analytically without first finding the elements of the ℓth row or column of $\overline{\overline{P}}$. However, we can examine the limiting behavior near and far from the carrier. Near the carrier, (30) gives

$$p_{\ell k} \approx \frac{-1}{\rho} \tag{32}$$

and substituting into (31) gives

$$\lim_{\omega\to 0} |\widetilde{\delta\theta}_{\text{total}}|^2 = |\widetilde{\delta\psi}_{\text{inj}}|^2. \tag{33}$$

Far from the carrier, we find

$$\sum_{i=1}^{N} p_{ij} = -\frac{\jmath\omega}{\omega_{3\text{dB}}} \tag{34}$$

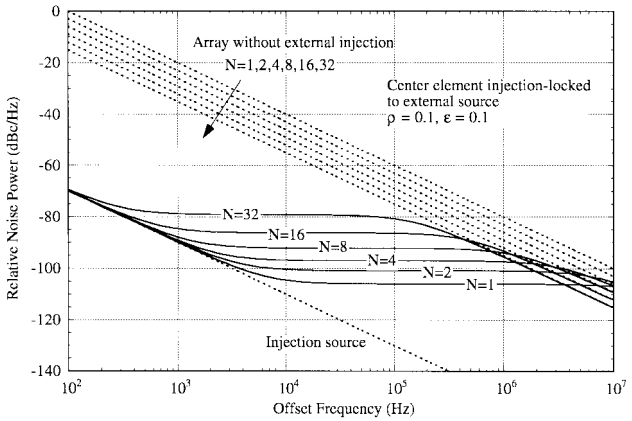

Fig. 6. Spectral characteristics of the phase noise in an array with the center element injection locked [Fig. 3(b)] for several array sizes, both with (solid line) and without (dotted line) the injected signal. The noise characteristics degrade with increasing array size.

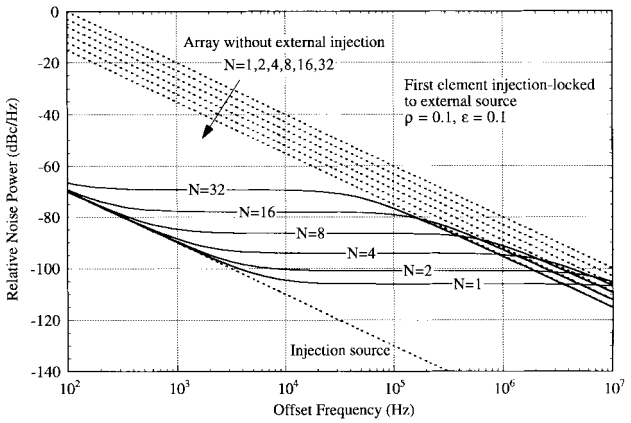

Fig. 8. Spectral characteristics of the phase noise in an array with the first element injection locked [Fig. 3(b)] for several array sizes, both with (solid line) and without (dotted line) the injected signal. The noise characteristics again degrade with increasing array size at a more rapid rate than Fig. 6.

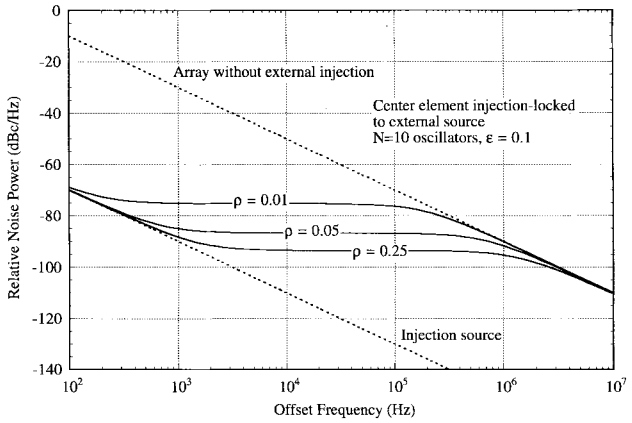

Fig. 7. Spectral characteristics of the phase noise in an array with the center element injection locked [Fig. 3(b)] versus normalized injection strength, for the specific case of $N = 10$.

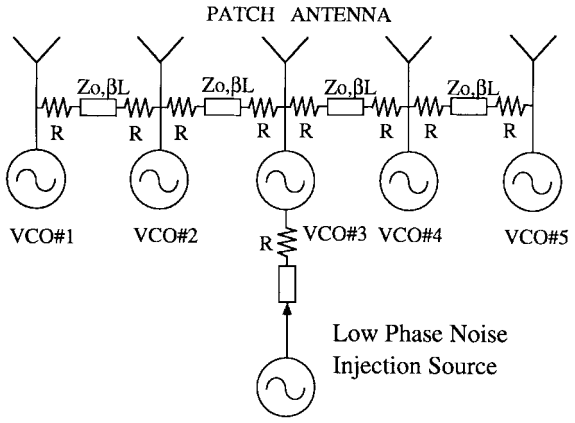

Fig. 9. Schematic of the experimental five-element array used in this work. The array operated in X-band, using packaged GaAs MESFET oscillators. See text and [2] and [11] for circuit details.

which gives

$$\lim_{\omega \to \infty} |\tilde{\delta\theta}_{\text{total}}|^2 = \frac{1}{N} |\tilde{\delta\theta}_0|^2. \tag{35}$$

These are the same asymptotic values as derived for the globally injected case. The behavior for intermediate frequencies is more computationally complicated, but qualitatively similar with respect to noise offset frequency. Fig. 6 illustrates the total phase noise as a function of the offset frequency for several different array sizes, with the injection signal applied to the center element. The same noise parameters of Fig. 6 were used as in Figs. 4 and 5, but a slightly larger injected signal strength was used ($\rho = 0.1$). Here we observe a significant degradation in the output phase noise with increasing array size. Fig. 7 illustrates the dependence on the injection strength. If the injection signal is instead applied at the first array element, the noise characteristics degrade more rapidly with increasing array size, as seen in Fig. 8. An analysis of the individual noise fluctuations on the array confirms that the individual contributions from the array elements increase with distance from the injected signal, at a rate that depends on the coupling strength. Thus, a practical system would clearly favor a large inter-oscillator coupling strength, a large injected signal strength, and the injected signal applied at the center of the array.

V. Experimental Results

A five-element linear coupled-oscillator chain was used for experimental verification of this paper's theory. This is shown in Fig. 9, and is a similar design to previously reported work [10]–[12]. The array is composed of five varactor-tuned MESFET voltage-controlled oscillators (VCO's) with a nominal tuning range of 8–9 GHz. These VCO's use NE32184A packaged MESFET's and MA-COM 46 600 varactor diodes, and are fabricated on the Rogers Duroid board 5880 ($\epsilon_r = 2.2$) with the thickness 0.787 mm. The VCO's are coupled together by one wavelength (at approximately $\omega_0/(2\pi) = 8.5$ GHz) microstrip transmission lines, resistively loaded with two 100-Ω chip resistors. As described in [10], this technique provides coupling parameters $\epsilon \approx 0.5$ and $\Phi = \beta L = 2\pi$. Each oscillator is designed to deliver power to a 50-Ω load. The oscillators were "connectorized" using SMA-

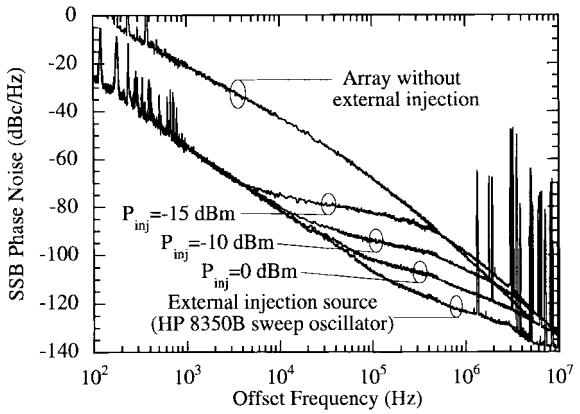

Fig. 10. Spectral characteristics of the phase noise of the experimental array. The results show good quantitative agreement with the theory, and qualitative agreement with the ideal curves of Fig. 7.

to-microstrip transitions, which allowed for simple testing and later connection to an external five-element patch-antenna array. The low-phase noise-source signal from an HP8350B sweep oscillator is injected into the center element by a 100-Ω chip resistor and a section of the microstrip transmission line. As described earlier, varying the end-element free-running frequencies induces a constant phase progression along the array. Representative radiation patterns for the experimental array are described in various end-element detunings [11]. When all elements are set to a common free-running frequency, the elements are nominally in phase and a broadside beam was detected. It was found that the array can remain locked within a maximum end-element detuning of approximately ± 125 MHz, which gives an estimation of the locking range $\Delta\omega_{\text{lock}/(2\pi)} = \epsilon\omega_0/(2\pi \cdot 2Q) = 125$ MHz; hence, Q factor $Q \approx 17$.

The same-phase noise-measurement apparatus in [2] was used to characterize both the total output array noise and the individual oscillator fluctuations in a variety of conditions. For total array noise, the oscillators were connected to a patch antenna array and the output signal was measured with a detector in the far field. Isolators were placed between the oscillator output and the antenna feed to maintain a 50-Ω load impedance when the oscillators were detuned for scanning. For the individual oscillator measurements, the oscillators were connected directly to the measurement system using SMA cables.

Fig. 10 shows the phase noise of the total array output under synchronized conditions (all oscillators set to a common free-running frequency), the noise of the injection source, and the array noise when locked to the injection source for three representative injection strengths. The injection-frequency was tuned to the oscillators' center frequency for the measurement. The results show good qualitative agreement with Fig. 7. In fact, using the measured values of the injection noise and free-running array noise [2], the theoretical curves computed using (21) were virtually indistinguishable from the measurement, and thus difficult to present on the same curve for comparison. Departures from the idealized curves of Fig. 7 are due to the more complicated frequency dependence of the array and injected noise sources.

VI. Conclusions

Analysis of the phase noise in coupled-oscillator array externally locked to a low phase noise source has been derived for the bilaterally coupled array. The analysis confirms that the phase noise of the array is approximately that of the injected source near the carrier, and approaches that of the free-running array far from the carrier. The general case involving arbitrary coupling topology of the array and injection signal is impossible to analytically solve, but can be easily treated numerically using the central result of the paper (21).

There are two important aspects of the array noise problem that have not been treated in this paper. The first is the influence of amplitude noise and possible conversion between amplitude and phase noise. The second is the effect of nonzero inter-element coupling phase and the resulting dependence of noise on the relative phasing of the oscillators. As discussed in [2], the phase noise near the locking band edge can markedly increase. Unfortunately, this problem is very complicated to treat analytically; the steady-state phase distribution for nonzero coupling phase must be solved using nonlinear root-finding algorithms, and there may be many solutions, each of which must be checked for stability. Some insight can be gleaned from the two-oscillator result (6), but the problem is probably best treated on a case-by-case basis. However, as we have shown in the experimental results of this and other papers [1], [10], [11], it is possible to minimize these effects by careful attention to the design of the coupling network.

Acknowledgment

The authors acknowledge the generous support of the California Eastern Labs, Los Angeles, CA, NEC Corporation, Los Angeles, CA, for donating the MESFET devices, and Rogers Corporation, Chandler, AZ, for donating the Duroid substrate material used in this paper. The authors also appreciate some helpful suggestions from the paper reviewers.

References

[1] J. J. Lynch, H.-C. Chang, and R. A. York, "Coupled-oscillator arrays and scanning techniques," in *Active and Quasi-Optical Arrays for Solid-State Power Combining*, R. A. York and Z. B. Popović, Eds. New York: Wiley, 1997, ch. 4, pp. 135–186.

[2] H.-C. Chang, X. Cao, U. K. Mishra, and R. A. York, "Phase noise in coupled oscillators: Theory and experiment," *IEEE Trans. Microwave Theory Tech.*, vol. 45, pp. 604–615, May 1997.

[3] S. Hamilton, "FM and AM noise in microwave oscillators," *Microwave J.*, vol. 21, pp. 105–109, June 1978.

[4] T. Makino, M. Nakajima, and J.-I. Ikenoue, "Noise reduction mechanism of power combining oscillator system," *Electron. Commun. in Japan*, vol. 62-B, no. 4, pp. 37–44, 1979.

[5] K. Kurokawa, "Injection locking of microwave solid-state oscillators," *Proc. IEEE*, vol. 61, pp. 1386–1410, Oct. 1973.

[6] R. Adler, "A study of locking phenomena in oscillators," *Proc. IRE*, vol. 34, pp. 351–357, June 1946 (reprinted *Proc. IEEE*, vol. 61, pp. 1380–1385, Oct. 1973).

[7] K. Kurokawa, "Noise in synchronized oscillators," *IEEE Trans. Microwave Theory Tech.*, vol. MTT-16, pp. 234–240, Apr. 1968.

[8] W. R. Day, G. E. Lindgren, and C. C. Peterson, "Microwave solid-state injection locked amplifiers," *Microwave J.*, vol. 19, no. 5, pp. 59–61, May 1976.

[9] H.-C. Chang, E. S. Shapiro, and R. A. York, "Influence of the oscillator equivalent circuit on the stable modes of parallel-coupled oscillators," *IEEE Trans. Microwave Theory Tech.*, vol. 45, pp. 1232–1239, Aug. 1997.

[10] R. A. York, P. Liao, and J. J. Lynch, "Oscillator array dynamics with broad-band N-port coupling networks," *IEEE Trans. Microwave Theory Tech.*, vol. 42, pp. 2040–2045, Nov. 1994.
[11] X. Cao and R. A. York, "Coupled oscillator scanning technique for receiver applications," in *IEEE AP-S Symp.*, Newport Beach, CA, 1995, pp. 1311–1314.
[12] H.-C. Chang, X. Cao, U. K. Mishra, and R. A. York, "Phase noise in coupled oscillator arrays," in *IEEE MTT-S Int. Microwave Symp. Dig.*, Denver, CO, June 1997, pp. 1061–1064.

Heng-Chia Chang received the B.S. degree in electrical engineering from National Taiwan University, Taipei, Taiwan, R.O.C., in 1990, the M.S. degree from the University of California at Santa Barbara (UCSB), in 1994, and is currently working toward the Ph.D. degree.

From 1990 to 1992, he served in the Air Force as a Technical Officer, stationed in Taiwan, where he received maintenance training about various wireless communication systems, GCA radar system, digital fiber-optical communication system, and digital PABX system. His current research interests include noise analysis, nonlinear microwave-circuit design, coupled oscillator theory, nonlinear optics, statistical optics, and quantum optics.

Xudong Cao received the B.S.E.E. degree from Beijing University of Aeronautics, Beijing, China, in 1982.

In 1982, he joined Luoyang Optical and Electrical Institute (LOEI), Henan, China, where he has been involved in the design of several microwave and millimeter-wave sources, and is currently a Senior Engineer. Since 1994, he has worked as a Visiting Researcher at the University of California at Santa Barbara (UCSB). He is currently engaged in the development of the low-phase noise frequency-agile source. His research interests are in the phase noise-reduction technique, noise theory of solid-state oscillators and devices, low-frequency noise measurement, and low-frequency noise in GaAs MESFET's.

Mark J. Vaughan (S'92–M'92) received the B.S. degree in electrical engineering from the California Institute of Technology, Pasadena, in 1991, and the M.S. and Ph.D. degrees in electrical engineering from Cornell University, Ithaca, NY, in 1993 and 1996, respectively.

He is currently a Research Scientist at Endgate Corporation, Sunnyvale, CA, where he develops millimeter-wave circuitry within a unique fabrication paradigm. His research interests include oscillator phase-noise and innovative planar millimeter-wave structures.

Dr. Vaughan is a member of Eta Kappa Nu and Tau Beta Pi.

Umesh K. Mishra received the B.Tech. degree in electrical engineering from the Indian Institute of Technology, Kanpur, India, in 1979, the M.S. degree in electical engineering from Lehigh University, Bethlehem, PA, in 1981, and the Ph.D. degree in electical engineering from Cornell University, Ithaca, NY, in 1984.

From 1983 to 1985, he was a Process Engineer at General Electric Company, Syracuse, NY. From 1985 to 1986, he was an Assistant Professor in the Department of Electrical Engineering and Computer Science, University of Michigan at Ann Arbor. In 1988, he was with Hughes Research Laboratories, as a Technical Staff Member. From 1989 to 1990, he was an Associate Professor at North Carolina State University. In 1991, he joined the faculty of the University of California at Santa Barbara (UCSB), where he is currently a Professor. His current research interests include semiconductor device physics, quantum electronics design and fabrication, optical control of microwave and millimeter-wave devices, nanometer fabrication techniques, *in-situ* processing, and integration techniques.

Dr. Mishra was awarded the Gledden Visiting Senior Fellowship from the University of Western Australia, Australia, in 1995. He was awarded the Junior Science Talent Scholarship in 1972, the National Science Talent Search Scholarship from the Government of India in 1974, the Best Project Award in electrical engineering for his B.Tech. thesis in 1979, and the Sherman Fairchild Fellowship from Lehigh University, in 1980. He was awarded the Presidential Young Investigator Award and the Young Scientist of the Year Award (International GaAs Symposium) in 1989 and 1990, respectively. He was the Principle Staff Engineer at the General Electric Company and IEEE Microwave Theory and Technique National Lecturer of Speakers Bureau in 1985 and 1988, respectively.

Robert A. York (S'85–M'89) received the B.S. degree in electrical engineering from the University of New Hampshire, Durham, in 1987, and the M.S. and Ph.D. degrees in electrical engineering from Cornell University, Ithaca, NY, in 1989 and 1991, respectively.

He is currently an Associate Professor of electrical and computer engineering, University of California at Santa Barbara (UCSB), where his group is currently involved with the design and fabrication of microwave and millimeter-wave circuits, microwave photonics, high-power microwave and millimeter-wave modules using spatial combining and wide-bandgap semiconductor devices, and time-domain modeling of antennas, power-combining arrays, and other electromagnetic or electronic structures.

Dr. York received the Army Research Office Young Investigator Award in 1993, and the Office of Naval Research Young Investigator Award in 1996.